Lowest Electronic Excited States of Poly(*para*-cyclobutadienylenecyclopentadienylcobalt)butadiynylene

B. Craig Harrison, J. M. Seminario, U. H. F. Bunz, and M. L. Myrick*

Department of Chemistry and Biochemistry, University of South Carolina, Columbia, South Carolina 29208

Received: August 24, 1999; In Final Form: February 9, 2000

The copolymer poly(*para*-cyclobutadienylenecyclopentadienylcobalt)butadiynylene was studied with electronic absorption, Raman, and resonance Raman spectroscopies to determine the nature of the lowest visible absorbance in the optical spectrum. The electronic absorption suggests the presence of two major transitions within 5000 cm^{-1} of one another in the lowest energy absorption band. Vibrational assignments were made by comparing the 457.9 nm excited resonance Raman frequencies and depolarization ratios to ab initio calculations, and enhancement values were calculated. Depolarization ratios show that the Raman enhancement of several modes results from two or more electronic transitions. These data show that the C−C triple bonds experience significant excited-state distortion in at least one of these transitions. However, we also find that several other vibration modes exhibit significant enhancement upon electronic excitation. These changes are consistent with a charge-transfer assignment for one of the lowest energy singlet excited states between a nonbonding butadiene-centered orbital and an antibonding conjugated orbital. Because of metal involvement in the nonbonding orbital, this transition has significant MLCT character. A second transition is suggested that may be localized on the metal complex portion of the molecules.

Introduction

In a previous report,[1] Bunz et al. studied the way in which properties of poly(*para*-cyclobutadienylenecyclopentadienylcobalt)butadiynylene (Figure 1) change with increasing chain length. In ref 1, the lowest energy visible absorbance (Figure 2) was assumed to be a $\pi \rightarrow \pi^*$ transition, analogous to other highly conjugated polymers[2]. These oligomers, however, are unique from most other highly conjugated polymers in several ways, among which are the presence of a transition metal ion and the interruption of the conjugated butadiyne backbone by strained cyclobutadiene rings. The presence of the nominally d^8 transition metal introduces the possibility of MLCT and LMCT transitions, as well as a periodic potential that perturbs the electron wave functions and could produce backbone-localized charge-transfer transitions between distinct portions of the backbone. The obvious test of whether the metal is involved significantly in the lowest energy transition would be to produce the polymer without the metal ion. Unfortunately, the transition-metal system is built into the oligomers precisely because of the instability of the compounds without it.

An alternative approach to elucidating the nature of the electronic transition responsible for the lowest energy visible absorbance of these molecules is to study the distortion of the vibrational modes of the molecule upon excitation. This could be most easily accomplished with high-resolution absorption spectroscopy. Unfortunately, the resolution of the vibronic structure of polymer electronic transitions is usually poor. In the case of these oligomers, the lowest absorbance exhibits only slight structure. An alternative approach is to use resonance Raman spectroscopy (RRS). RRS has been used extensively to study the vibronic nature of electronic transitions.[3−19] In particular, photoinduced charge-transfer transitions such as LMCT, MLCT, LLCT, and charge transfer in inorganic and organic donor−acceptor complexes have been studied.[8−19]

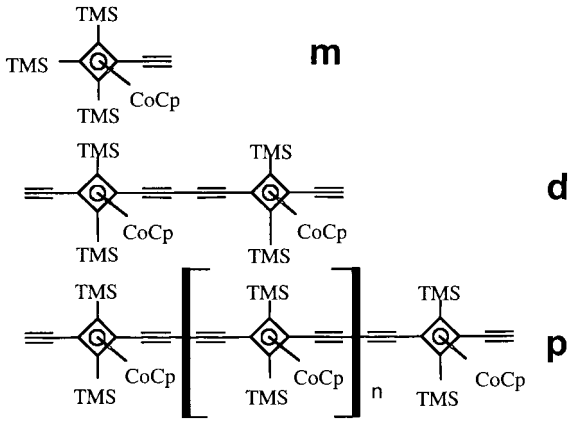

Figure 1. Structures of the monomer (top), dimer (middle), and polymeric (bottom) forms of (*para*-cyclobutadienylenecyclopentadienylcobalt) butadiynylene.

The present manuscript reports the results of our effort to elucidate the nature of the electronic transition behind the lowest energy visible absorbance of the poly(*para*-cyclobutadienylenecyclopentadienylcobalt)butadiynylene polymer using resonance Raman spectroscopy. To accomplish this, we rely on ab initio vibrational frequency calculations to help us assign the major Raman and resonance Raman frequencies, and then calculate enhancements for the major resonance-enhanced modes. These assignments and calculations appear consistent with a charge-transfer assignment for the lowest energy absorbance with significant MLCT character.

Experimental Section

Raman and resonance Raman spectra were acquired of dissolved oligomeric samples. For these measurements, reagent

* To whom correspondence should be addressed. E-mail: myrick@psc.sc.edu. Fax: 803 777 9521.

10.1021/jp9930200 CCC: $19.00
Published on Web 06/01/2000

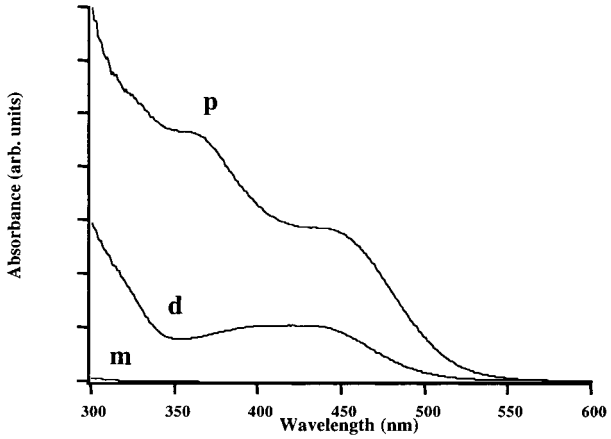

Figure 2. Electronic absorption spectra of monomer, dimer, and polymer. Spectra were acquired in carbon tetrachloride solvent at room temperature. The curve labels are p, d, and m for polymer, dimer, and monomer, respectively.

grade CCl_4 (Aldrich Chemical Co.) was used as both a solvent and as an internal standard for the calculation of enhancement values. Samples were prepared of the polymer (1,900 g/mol), dimer, and monomer by dissolving appropriate amounts of solid into 1 dram vials filled with CCl_4. Because of inner filter effects, sample concentrations were varied to find the maximum solute Raman intensity. After the Raman spectra were acquired, sample concentration was back-calculated from a calibration curve based on the electronic absorption spectroscopy of standards. For measurements excited at 457.9 nm, the typical solution concentrations of analyte were 1 mM for the monomer, 20 μM for the dimer, and 5 μM for the polymer. Measurements excited at 785 nm were made on samples with concentrations 100× larger than those at 457.9 nm and an excitation power 3.33× higher.

UV−Vis absorption spectroscopy was performed in room-temperature fluid solutions on a Perkin-Elmer, Inc. Lambda 14 UV−Vis spectrophotometer controlled by a Hewlett-Packard computer running UV WinLab 2.70.01.

The resonance Raman spectra were excited at 457.9 nm by a Coherent Innova 300 CW Argon ion laser. The laser power at the fluid sample surface was measured to be 90 mW. The laser light was focused onto the top of the solution to avoid passing through a window, and Raman-scattered light was collected at 180° to reduce sample reabsorption of the scattering. The light was collected and focused into a Chromex 250 IS imaging spectrograph equipped with an 1800 grooves/mm grating blazed at 500 nm. A Princeton Instruments Inc. TE/CCD-1100-PF 1100 × 330 element CCD array thermoelectrically cooled to −50 °C was used for detection. The detector was controlled with WinSpec version 1.6.2 software from Princeton Instruments. The entrance slit width of the spectrograph was set at 125 μm, giving a resolution between 8 and 9.4 cm^{-1} across the total range over which the spectroscopy was measured. For depolarization ratio measurements, the exciting light was passed through a Coherent 03PBB007 broadband polarizing beam splitter cube to clean up the polarization of the excitation source, and the scattered light was passed through an Ealing 23−5671 polarizer, and a Coherent 43−8655 depolarizer before reaching the spectrograph. The depolarizer was used to negate any polarization dependence of the spectrograph.

Raman spectra were obtained off-resonance using a Spectra Diode Labs Model SDL-8530 CW external cavity diode laser. The laser emitted 785 nm light with a power of 300 mW at the sample. The optics for this experiment were identical to those for resonance Raman, except that both a 1200 grooves/mm grating blazed at 750 nm and a 300-grooves/mm grating blazed at 1000 nm were used for dispersion. The entrance slit width for these experiments was set to 150 μm giving a resolution between 4.6 and 5.6 cm^{-1} and 16 to 18.5 cm^{-1} for the two gratings, respectively.

The polymer was used as provided by the Bunz laboratory. Despite intense excitation into the lowest energy visible absorbance of the compounds, no evidence for photodecomposition of the samples by the laser was observed. Spectral waveforms were independent of laser power, and remained unchanged with exposure to the laser for 2−5 min. The only circulation of the sample was through convective mixing.

Spectral corrections to subtract out solvent peaks and polynomial-fitted fluorescence baselines were made using Wavemetrics Inc. Igor Pro Version 3.13. Also Igor Pro was used to calibrate the wavenumber scale for each spectrum based on a polynomial fit to a toluene standard. The toluene used as the standard was E M Science reagent grade toluene used as received from the company. The wavenumber scale values for toluene frequencies were obtained from the 50/50 toluene/acetonitrile ASTM E 1840 Raman Shift Standard supplemented with values taken from a spectrum of toluene taken using a Perkin-Elmer 1700X NIR FT-Raman spectrometer.

Ab Initio Calculations. The Gaussian-94[20] program was used to estimate both the dimer and the monomer vibrational modes. The raman active modes were characterized. Full optimizations using the highest possible point group were performed using the Hartree−Fock method. The minimal STO-3G basis set was used for the monomer and dimer, and the 3-21G was also used for the monomer.

Results and Discussion

The electronic spectroscopy of the molecules in question is presented in Figure 2. Examination reveals that the low-energy absorption maxima are in the UV (monomer) or 450-nm region (dimer and polymer), and that those maxima are only poorly resolved. An ideal application of resonance Raman spectroscopy to this problem would utilize several excitation wavelengths in an effort to elucidate the enhancement profile. Unfortunately, our laboratory is limited to the most common argon ion laser wavelengths for visible excitation. Of these, only the 457.9 nm line is strongly absorbed by the dimer and polymer and gives rise to strong enhancement. Single-wavelength excitation limits the following analysis because we cannot obtain enhancement profiles for the multiple-state transitions that appear to occur in the dimer and polymer. In the case of the dimer, for example, the lowest energy absorbance is clearly a summation of at least two transitions with significant intensity separated by less than 5000 cm^{-1}.

Resonance Raman. Resonance Raman spectroscopy of the monomer, dimer, and polymer excited at 457.9 nm are shown in Figure 3, with 785-nm-excited Raman spectra of the same compounds shown in Figure 4. The 785-nm-excited Raman spectra were obtained in the hope that more frequencies would be observed to aid in assignment. Depolarization ratios, ρ, were defined as shown in eq 1.

$$\rho = \frac{I_{\perp}}{I_{\parallel}} \tag{1}$$

Depolarization ratios, based on peak areas, were measured for all of the major peaks in the 457.9 nm excited resonance Raman spectra, and these are given in Table 1. Despite the 100-fold

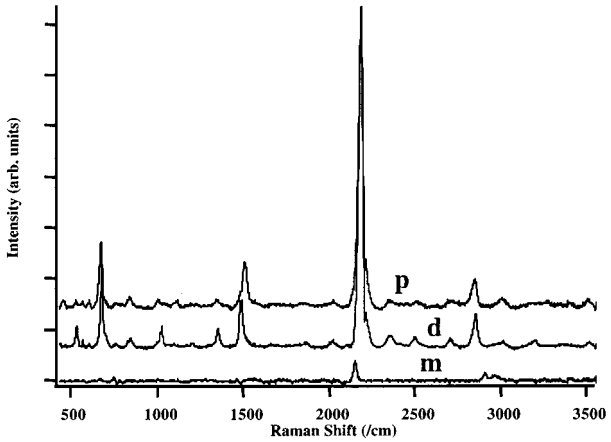

Figure 3. Resonance Raman spectroscopy of monomer, dimer, and polymer excited at 457.9 nm. The curve labels are p, d, and m for polymer, dimer, and monomer, respectively.

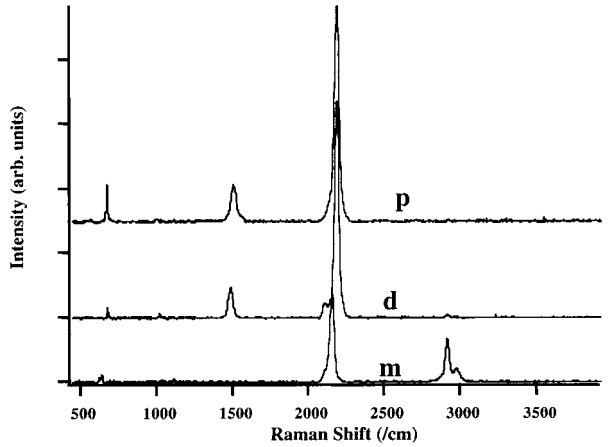

Figure 4. Raman spectroscopy of the monomer, dimer, and polymer excited at 785 nm. The curve labels are p, d, and m for polymer, dimer, and monomer, respectively.

TABLE 1: Measured Resonance Raman Frequencies and Depolarization Ratios for Raman Modes of the Monomer, Dimer, and Polymer. All Data are for 457.9 nm Excited Raman Spectra

sample	frequency (cm^{-1})	depolarization ratio
monomer	2152	0.119
2905	0.100	
dimer	528	0.328
672	0.269	
840	0.438	
1021	0.266	
1479	0.267	
2014	0.410	
2181	0.349	
2850	0.483	
polymer	667	0.355
1501	0.435	
2181	0.364	
2843	0.488	

lower concentration of the analytes used for the resonance Raman measurements, the spectrum of the solvent (CCl_4, not shown) is significantly reduced in relative intensity in these spectra compared to the near-IR-excited measurements. Similarly, the Raman spectrum of the monomer is significantly weaker than the spectra of the dimer and polymer. This is despite the higher concentration of the monomer and the fact that there is no inner filtering of either the excitation or the scattering excited at 457.9 nm for the monomer. We conclude that all of the frequencies observed in the 457.9 nm excited dimer and polymer spectra are enhanced compared to their 785-nm-excited spectra, and they are likewise enhanced compared to the monomer through a resonance process.

When excitation is into a single electronic transition, common depolarization ratios observed for resonance-enhanced Raman modes are $^1/_8$ (degenerate states) and $^1/_3$ (nondegenerate states).[21] Other values indicate the presence of more than one electronic state with different transition dipole directions. The values between $^1/_3$ and $^3/_4$ are characteristic of overlapping electronic transitions for cases in which the excitation is between the two electronic origins.[22,23] The depolarization ratios that we report for the dimer and polymer all range between 0.27 and 0.48. Our estimated error in these measurements is less than 0.1, so these differences are significant. Several of the frequencies observed for the dimer and polymer possess depolarizations near $^1/_3$, an indication that the enhancement for these Raman frequencies can be explained by a single electronic state (or more than one state with the same transition dipole direction).[24] We observe, however, that three Raman modes of the dimer and two of the polymer are observed with depolarizations greater than or equal to 0.4, requiring a multiple state origin.

Absorbance. Referring to Figure 2, we observe that the monomeric species has relatively little absorbance in the visible compared to the dimer and polymer. Reference 1 shows that the monomer has major absorbances at 247 and 298 nm. Of these, only part of the latter is observed in Figure 2. With increasing conjugation length, a bathychromic shift of the lowest energy absorbance due to $\pi-\pi^*$ transitions is expected. The dimer and polymer, however, have similar lowest energy absorption features despite a significantly greater conjugation length for the latter. One obvious difference between the spectra of the dimer and polymer is the shift of the second-lowest-energy absorption maximum from approximately 330 nm**1** to 370 nm. This could indicate that the lowest absorbance is not the anticipated $\pi-\pi^*$ transition but some transition less sensitive to conjugation length. Alternatively, the π-conjugation of the polymer could be disrupted by the presence of the metal ions in these compounds, and this could result in a smaller red shift than would be expected.

Because of the low resolution of the absorption features in the electronic spectroscopy of these molecules, we turn to the Raman and resonance Raman spectroscopy as an aid in assigning the electronic origins of the lowest energy absorbance.

Peak Assignments. The complexity of the molecules under study necessitated that mode assignments rely to a large extent on ab initio calculations for the relatively few vibrations observed. A summary of the calculated frequencies for the various modes is provided in Table 2.

Using the observed depolarization ratios and the calculated vibrational frequencies and symmetries as a guide, we have assigned some of the major observed vibrational modes as shown in Table 3.

The 2152 cm^{-1} mode of the monomer observed in the 457.9 nm excited spectrum is replaced by a peak at 2181 cm^{-1} in the dimer and polymer. The only vibrations of the molecule that are likely to have frequencies in this range are the C−C triple-bond stretches. In the monomer, there is only one such vibration, whereas in the dimer, there are two. There are increasing numbers of symmetrically inequivalent butadiynyl units as the oligomer length increases. However, we can expect the terminal ethynyl unit to be significantly different from the internal butadiynyl groups, whereas the internal butadiynyls are likely to be similar to one another. Hence, although the 2152 cm^{-1} mode of the monomer must belong to a terminal ethynyl unit,

TABLE 2: Most Prominent Vibrational Modes of the Monomer and Dimer Found by ab Initio Calculations

sample	frequency (cm^{-1})	assignment
monomer	592	chain rocking
641	CB twist	
737	chain rocking	
946	asymmetric CB stretch	
1070	Cp ring breathing	
1158	asymmetric CB stretch	
1309	asymmetric Cp stretch	
1399	symmetric Cb stretch	
2132	terminal C≡C stretch	
2891	asymmetric CH_3 stretch	
2900	CH symmetric stretch (TMS)	
3065	CH symmetric stretch (Cp)	
3253	asymmetric terminal CH stretch	
dimer	484	chain rocking
560	asymmetric stretch of CB ring	
579	Cp and CB ring deformation	
695	Si − C symmetric stretch	
785	asymmetric stretch of CB ring	
1038	asymmetric stretch of Cp ring	
1151	symmetric stretch of Cp ring	
1191	asymmetric stretch of CB ring	
1430	CB − C stretch along backbone	
1500	CB ring breathing	
1502	asymmetric CH_3 stretch	
1651	CH_3 bending	
2359	terminal C≡C stretch	
2516	internal C≡C stretch	

TABLE 3: Observed Raman Frequencies and Assignments for the Monomer, Dimer, and Polymer.

vibrational assignment	monomer frequency	dimer frequency	polymer frequency
−Si−CH_3 stretch	696	676[b]	670[b]
pentadiene ring-breathing	N. Obs.	1025[b]	1013[b]
butadiene ring-breathing	N. Obs.	1481[b]	1500[b]
terminal C≡C stretching	2152	2113	N. Obs.
interior C≡C stretch	N. A.	2181[b]	2183[b]
C−H stretch (TMS)	N. Obs.	2850[b]	2843[b]
C−H stretch (TMS)	2910	2920	N. Obs.
antisymmetric C−H stretch (terminal TMS)	2972	N. Obs.	N. Obs.

[a] The unobserved modes are labeled "N. Obs.", whereas those that are not present in the monomer are labeled "N. A." [b] The mode is observed in the resonance Raman spectrum.

the dimer and polymer could have at least two distinct alkyne vibrational frequencies. In the polymer, the terminal ethynyl unit comprises only a small fraction of the alkynes; hence, the observed RR-enhanced mode is likely the interior butadiynyl stretching frequency. The dimer, in its 785-nm-excited spectrum, shows two closely spaced modes, one at 2181 cm^{-1}, matching the RRS-enhanced frequency, and a weaker mode at 2105 cm^{-1}. By extension from the polymer, the 2181 cm^{-1} mode observed in the RRS of the dimer is therefore assigned as the interior butadiynyl stretching frequency, whereas the less intense mode observed in the 785-nm-excited spectra is assigned as the stretching of the terminal triple bonds.

Only one mode appears exclusively in the 785-nm-excited Raman spectrum, and that is the 2972 cm^{-1} vibration of the monomer. An assignment as an antisymmetric C−H stretch of TMS methyl groups is most consistent with a mode at this frequency. However, this vibration does not appear in either the dimer or the polymer. Because the dimer and polymer differ from the monomer by the lack of a terminal TMS group and because the monomer has two distinct types of TMS groups that are symmetrically inequivalent, we conclude that the terminal TMS group of the monomer is responsible for this Raman-active mode.

TABLE 4: Calculated Enhancement Factors for Major Observed Resonance Raman Frequencies in Figure 3

sample	peak (cm^{-1})	enhancement
monomer	2152	1.04×10^4
2905	7.27×10^3	
dimer	528	8.39×10^4
672	3.02×10^5	
1021	4.71×10^4	
1479	2.00×10^5	
2181	1.79×10^6	
2850	1.97×10^5	
polymer	667	9.83×10^5
1501	1.06×10^6	
2181	7.71×10^6	
2843	8.62×10^5	

RRS Enhancements. Resonance Raman is performed similarly to normal Raman spectroscopy, with the exception that the energy of excitation is selected to correspond to an electronic absorbance of the molecules under study. During the time in which the photon and molecule interact, the system samples the molecular excited state(s) at the photon's energy above the ground state. The scattering of a Raman-scattered photon depends on the Franck−Condon overlap of a vibrationally excited ground state with the coherent wave packet of the photon−molecule system and, hence, on the displacement between the potential energy surfaces of ground and excited state(s).

Several methods have been developed for relating the observed intensities of resonance Raman emissions to the excited-state vibrational displacement of the molecule relative to the ground state.[25−33] Qualitatively, all of the available methods for interpreting RRS relate the mode displacements of excited molecules to the observed enhancement factors, but the relationship is not quantitatively linear. One of the simplest methods that can be applied is the transform method.[28,31−33] The transform method works best when a full resonance Raman excitation profile can be obtained and when excitation is to a single state. Unfortunately, our laboratory is not equipped with sufficient blue and UV wavelengths to examine the high-energy side of the lowest absorbance in these molecules. Furthermore, evidence from depolarization measurements indicates that more than a single state is involved in the enhancement of the observed modes. We have thus relied on the more qualitative analysis based on relative enhancements.

The resonance Raman enhancements for the vibrations of the monomer, dimer, and polymer that exhibited the greatest enhancement were calculated by comparison to the solvent, CCl_4, mode intensities. R_e, the resonance Raman enhancement of the sample modes, is given by eq 2,

$$R_e = \frac{I_{samII} + 2I_{sam\perp}}{I_{CCl_4II} + 2I_{CCl_4\perp}} * \frac{1}{\chi_{sam}} \qquad (2)$$

where R_e is the resonance enhancement, I_{samII}, $2I_{sam\perp}$, I_{CCL_4II}, and $2I_{CCl_4\perp}$ are the integrated intensities of the parallel polarized sample peak, perpendicularly polarized sample peak, parallel polarized 318 cm^{-1} peak of CCl_4, and the perpendicularly polarized 318 cm^{-1} peak of CCl_4, respectively, and χ_{sam} is the mole fraction of the sample in solution. The results of these calculations are provided in Table 4.

Orbitals. The electronic structure of the backbone of these compounds can be considered, in a first approximation, as if it were composed of modified cyclobutadiene (CB) groups connected by alkene linkages because of the local symmetry defined by the CB rings. The $\pi-\pi^*$ transitions belonging to the in-

plane π orbitals of the butadiynyl moieties are, thus, at too high an energy to be observed in our spectroscopic measurements and are of little concern to us. The valence orbitals of the CB−Co−Cp group in these compounds have been the subject of at least two theoretical studies.[34,35] Of these, ref 34 gives the more detailed results, and from their work, it is clear that only four (labeled 13a′, 16a′, 17a′, and 10a″ under the C_s labels, in order of increasing energy) have significant cyclobutadiene character.

Of the orbitals with π_{CB} character, three would participate significantly in π-bonding with the butadiynyl linkages, leaving one of the two highest lying filled orbitals unchanged. The two highest lying filled orbitals of the CB−Co−Cp unit are both nonbonding in the CB subunit. Of these two, it is the 10a″ orbital that should remain essentially nonbonding in character upon attachment of the butadiynyl linkage, using the nomenclature of ref 34. The remaining orbital, 17a′, will couple strongly with the out-of-plane π orbitals of an butadiynyl group on the ring. π-bonding possibilities between the cyclobutadiene ring due to the attached trimethylsilanes complicate matters somewhat.

These observations from theory permit an interpretation of the results obtained in the present work. As mentioned above, the alkyne vibrations of the interior butadiynyl groups exhibit large enhancement upon resonance excitation. This can be interpreted to mean that the optical transition in resonance at 457.9 nm distorts the triple bonds of the interior butadiynyl groups. We conclude that the LUMO, the HOMO, or a nearly-degenerate orbital in the dimer and polymer contain appreciable electron density in π-type orbitals of the butadiyne units.

We also find that significant enhancement of the C−H stretch of the TMS groups, the Si−CH_3 stretches, the CB ring-breathing mode and the Cp^- ring-breathing mode occurs. When we compare the distortions implied by these enhancements to the description of the orbitals in ref 34, we conclude that the other orbital involved in one of the lowest energy transitions is likely similar to the nominally non-bonding orbital given the designation 10a″ in the reference but connected by π-bonding to the TMS groups. Using the nonbonding nature of this orbital as a guide, it likely forms the HOMO of the dimer and polymer. This orbital has significant metal character to it and, thus, provides the lowest energy transition with some MLCT character.

We note that the 840, 2014, and 2181 cm^{-1} modes of the dimer and the 1501 and 2843 cm^{-1} modes of the polymer have depolarizations (Table 1) that imply the involvement of at least one additional electronic transition. The assignments that the authors have made of this set of vibrations suggests that they are all or mostly associated with the CB portion of the molecules. Because the C−C triple bond vibrations exhibit depolarizations of $^1/_3$ (within our experimental error), this suggests that the second state providing resonance enhancement is localized to the CB−Co−Cp units.

Conclusions

Using a combination of electronic absorption, Raman, and resonance Raman spectroscopies, augmented by ab initio calculations of vibrational frequencies and consistent with literature calculations, we find that the lowest electronic absorption bands of the copolymer poly(*para*-cyclobutadienylenecyclopentadienylcobalt) butadiynylene result from at least two distinct electronic transitions. One of these transitions may be partly MLCT in character, and the results imply that a second transition may be localized to the metal-complex portions of the molecules. Our experimental apparatus limits our investigation so that our data does not lead to a direct conclusion about which of these transitions is lowest in energy. Comparison of the dimer and polymer to the monomer, however, suggests that a CB−Co−Cp^--centered transition, even when perturbed by electron-donating butadiyne linkages, should be higher in energy than the lowest energy absorbance of the dimer and polymer.

Acknowledgment. The authors would like to thank the National Science Foundation, through Grant No. EPS-9630167, and the Office of Naval Research, through Grant No. N00014-97-1-0806, for support. B.C.H. would also like to thank the South Carolina EPSCoR office for summer support for this work. J.M.S. thanks NASA for supercomputer support. U.H.F.B. thanks the Petroleum Research Fund for support.

References and Notes

(1) Altmann, M.; Enkelmann, V.; Beer, F.; Bunz, U. H. F. *Organometallics* **1996**, *15*, 394
(2) Streitwieser, A. *Molecular Orbital Theory for Organic Chemists*; Wiley: New York, 1961; p 207.
(3) Asher, S. A.; Chi, Z. H.; Li, P. S.; *J. Raman Spectrosc.* **1998**, *29*, 927.
(4) Schnepf, R.; Sokolowski, A.; Muller, J.; Bachler, V.; Wieghardt, K.; Hildebrandt, P.; *J. Am. Chem. Soc.* **1998**, *120*, 2352.
(5) Aarnts, M. P.; Wilms, M. P.; Stufkens, D. J.; Baerends, E. J.; Vleck, A.; *Organometallics* **1997**, *16*, 2055.
(6) Holtz, J. S. W.; Bormett, R. W.; Chi, Z. H.; Cho, N. J.; Chen, X. G.; Pajicini, V.; Asher, S. A.; Spinelli, L.; Owen, P.; Arrigoni, M. *Appl. Spectrosc.* **1996**, *50*, 1459.
(7) Bettermann, H.; Dasting, I.; Rauch, W. *J. Chem. Phys.* **1993**, *99*, 1564.
(8) Webb, M. A.; Kwong, C. M.; Loppnow, G. R. *J. Phys. Chem. B* **1997**, *101*, 5062.
(9) Choi, C. L.; Phillips, D. L. *Mol. Phys.* **1997**, *94*, 547.
(10) Wright, P. G.; Stein, P.; Burke, J. M.; Spiro, T. G. *J. Am. Chem. Soc.* **1979**, *101*, 3531.
(11) Doorn, S. K.; Hupp, J. T. *J. Am. Chem. Soc.* **1989**, *111*, 4704.
(12) Maruszewski, K.; Bajdor, K.; Strommen, D. P.; Kincaid, J. R. *J. Phys. Chem.* **1995**, *99*, 6286.
(13) Wootton, J. L.; Zink, J. I. *J. Phys. Chem.* **1995**, *99*, 7251.
(14) Williams, R. D.; Petrov, V. I.; Lu, H. P.; Hupp, J. T. *J. Phys. Chem.* **1997**, *101*, 8070.
(15) Doorn, S. K.; Hupp, J. T. *J. Am. Chem. Soc.* **1989**, *111*, 1142.
(16) Wang, C.; Mohney, B. K.; Williams, R. D.; Petrov, V. I.; Hupp, J. T.; Walker, G. C. *J. Am. Chem. Soc.* **1998**, *120*, 5848.
(17) Britt, B. M.; McHale, J. L.; Friedrich, D. M. *J. Phys. Chem.* **1995**, *99*, 9, 6347.
(18) Kulinowski, K.; Gould, I. R.; Myers, A. B. *J. Phys. Chem.* **1995**, *99*, 9017.
(19) Markel, F.; Ferris, N. S.; Gould, I. R.; Myers, A. B. *J. Am. Chem. Soc.* **1992**, *114*, 6208.
(20) Frisch, M. J.; Trucks, G. W.; Schlegel, H. B.; Gill, P. M. W.; Johnson, B. G.; Robb, M. A.; Cheeseman, J. R.; Keith, T.; Petersson, G. A.; Montgomery, J. A.; Raghavachari, K.; Al-Laham, M. A.; Zakrzewski, V. G.; Ortiz, J. V.; Foresman, J. B.; Ciolowski, J.; Stefanov, B. B.; Nenayakkara, A.; Challacombe, M.; Peng, C. Y.; Ayala, P. Y.; Chen, W.; Wong, M. W.; Res, J. L.; Replogle, E. S.; Gomperts, R.; Martin, R. L.; Fox, D. J.; Binkley, J. S.; Defrees, D. J.; Baker, J.; Stewart, J. P.; Head-Gordon, M.; Gonzalez, C.; Pople, J. A. Gaussian 94, Revision E.1; Gaussian, Inc.: Pittsburgh, PA, 1996.
(21) Strommen, D. P. *J. Chem. Educ.* **1992**, *69*, 803.
(22) Shang, Q.-Y.; Hudson, B. S. *Chem. Phys. Lett.* **1992**, *183*, 63.
(23) Henneker, W. H.; Penner, A. P.; Siebr, W.; Zgierski, M. Z *J. Phys. Chem.* **1978**, *69*, 1704.
(24) *Laser Techniques in Chemistry*; Myers, A. B., Rizzo, T. R. Ed.; Wiley: New York, 1995; p 325.
(25) Kramers, H. A.; Heisenburg, W. *Z. Phys.* **1925**, *31*, 681.
(26) Dirac, P. A. M. *Proc. R. Soc.* (*London*) **1927**, *114*, 710.
(27) Manneback, I. *Physica* **1951**, *17*, 1001.
(28) Hizhnyakov, V.; Tehver, I. *Phys. Status. Solidi* **1967**, *21*, 755.
(29) Lee, S. Y.; Heller, E. J. *J. Chem. Phys.* **1979**, *71*, 4777.
(30) Heller, E. J.; Sundberg, R. L.; Tannor, D. *J. Phys. Chem.* **1982**, *86*, 1822.
(31) Tonks, D. L.; Page, J. B. *Chem. Phys. Lett.* **1979**, *66*, 449.
(32) Blazej, D. C.; Peticolas, W. L. *J. Chem. Phys.* **1980**, *72*, 3134.
(33) Stallard, B. R.; Champion, P. M.; Callis, P. R.; Albrecht, A. C. *J. Chem Phys.* **1983**, *78*, 712.
(34) Gleiter, R.; Hyla-Kryspin, I.; Binger, P.; Regitz, M. *Organometallics* **1992**, *11*, 177.
(35) Clark, D. W.; Warren, K. D. *Inorg. Chim. Acta* **1978**, *27*, 105.